

NEONATAL JAUNDICE

Bilirubin enhances the activity of ASIC channels to exacerbate neurotoxicity in neonatal hyperbilirubinemia in mice

Ke Lai^{1*}, Xing-Lei Song^{2*}, Hao-Song Shi^{1*}, Xin Qi², Chun-Yan Li¹, Jia Fang¹, Fan Wang¹, Oleksandr Maximyuk³, Oleg Krishtal³, Tian-Le Xu², Xiao-Yan Li⁴, Kun Ni⁴, Wan-Peng Li⁴, Hai-Bo Shi^{1†}, Lu-Yang Wang^{5,6†}, Shan-Kai Yin^{1†}

Neonatal hyperbilirubinemia is a common clinical condition that can lead to brain encephalopathy, particularly when concurrent with acidosis due to infection, ischemia, and hypoxia. The prevailing view is that acidosis increases the permeability of the blood-brain barrier to bilirubin and exacerbates its neurotoxicity. In this study, we found that the concentration of the cell death marker, lactate dehydrogenase (LDH) in cerebrospinal fluid (CSF), is elevated in infants with both hyperbilirubinemia and acidosis and showed stronger correlation with the severity of acidosis rather than increased bilirubin concentration. In mouse neonatal neurons, bilirubin exhibits limited toxicity but robustly potentiates the activity of acid-sensing ion channels (ASICs), resulting in increases in intracellular Ca²⁺ concentration, spike firings, and cell death. Furthermore, neonatal conditioning with concurrent hyperbilirubinemia and hypoxia-induced acidosis promoted long-term impairments in learning and memory and complex sensorimotor functions *in vivo*, which are largely attenuated in ASIC1a null mice. These findings suggest that targeting acidosis and ASICs may attenuate neonatal hyperbilirubinemia complications.

INTRODUCTION

Neonatal hyperbilirubinemia, the elevated concentration of serum bilirubin, has been known to damage neural function and morphology (1–3). Accumulation of bilirubin in the central nervous system (CNS) results in neurotoxicity in areas such as the ventral cochlear nucleus, vestibular nuclei, cerebellum, and hippocampus (4). Bilirubin cytotoxicity can be exacerbated during neonatal life by genetic mutations of key enzymes that are required for its metabolism and clearance (5, 6) and/or by comorbidities with other complications, for example, concurrent hyperbilirubinemia and acidosis (7). The current prevailing hypothesis is that acidosis alters the permeability of the blood-brain barrier (BBB), resulting in the accumulation of bilirubin in the brain (8–11). However, there is lack of solid clinical evidence and mechanistic insight linking concurrent hyperbilirubinemia and acidosis to increased cell death. Understanding their interactions holds the potential for identifying molecular substrates as alternative targets to protect the developing brain from injury during hyperbilirubinemia and acidosis.

Acidification due to ischemia and hypoxia can directly activate acid-sensing ion channels (ASICs), members of the degenerin/epithelial sodium channel superfamily (12, 13). These channels form homo- or heterotrimers of the ASIC subunits: 1a, 1b, 2a, 2b, 3, and 4, among which ASIC1a, 2a, and 2b are the major subunits found in the CNS (14–16). Depending on the assembly, functional channels vary their

half-maximal activation pH values (pH₅₀) and ionic permeability (17). ASICs are thought to be involved in acidosis-mediated cell death in ischemic brain injury (18–20). Despite the current conceptual paradigm that acidosis can enhance the overload of bilirubin to the neonatal brain (11, 21), the reciprocal relationship between bilirubin- and ASIC-dependent neurotoxicity remains unknown.

In this study, we examined the relationships between blood pH, bilirubin concentration, and concentration of lactate dehydrogenase (LDH) in the cerebrospinal fluid (CSF) (a marker for cell death) from infants in the intensive care unit. We found that neonates experiencing hyperbilirubinemia concurrent with acidosis have an increased concentration of LDH compared with patients with either condition alone, suggesting a synergistic neurotoxicity. By applying patch-clamp electrophysiology, Ca²⁺ imaging, and cell death assays to the medial vestibular nucleus (MVN) neurons of neonatal mice, we demonstrated that bilirubin exhibited marginal neurotoxicity on its own, but potentiated the currents mediated by ASIC1a channels in an acidic environment via Ca²⁺-dependent intracellular signaling, and jointly boosted neuronal excitability, Ca²⁺ overload, and cell death. Consistent with these results *in vitro*, neonatal conditioning with concurrent hyperbilirubinemia and acidosis primed long-term impairment of sensory and cognitive deficits *in vivo* in mice. Our findings offer translational insights into the molecular mechanisms underlying aggravated neurotoxicity in neonatal brains with hyperbilirubinemia and acidosis, suggesting possible therapeutic targets for clinical intervention of neonatal hyperbilirubinemia.

RESULTS

Cross-correlation analyses of blood bilirubin and pH with LDH in infant CSF with hyperbilirubinemia and/or acidosis

To quantitatively investigate the relationship between the concentration of blood bilirubin, pH, and cell damage/death, we collected data from a total of 162 infants with hyperbilirubinemia and/or acidosis

¹Department of Otorhinolaryngology, Sixth People's Hospital of Shanghai and Shanghai Jiao Tong University, Shanghai 200032, China. ²Department of Anatomy and Physiology, Shanghai Jiao Tong University School of Medicine, Shanghai 200025, China. ³Bogomoletz Institute of Physiology of NAS Ukraine, Kyiv 01024, Ukraine. ⁴Department of Otorhinolaryngology, Shanghai Children Hospital and Shanghai Jiao Tong University, Shanghai 200062, China. ⁵Program in Neuroscience and Mental Health, SickKids Research Institute, Toronto M5G 1X8, Canada. ⁶Department of Physiology, University of Toronto, Toronto M5S 1A1, Canada.

*These authors contributed equally to this work.

†Corresponding author. Email: hbshi@sjtu.edu.cn (H.-B.S.); luyang.wang@utoronto.ca (L.-Y.W.); skyin@sjtu.edu.cn (S.-K.Y.)

who had undergone examination of CSF-LDH, an established marker of brain tissue damage. The patients were divided into three cohort groups based on diagnostic criteria for acidosis (group 1), hyperbilirubinemia (group 2), and confounding acidosis and hyperbilirubinemia (group 3) (fig. S1 and table S1). Statistical analyses with the Dunnett T3 test indicated that the mean CSF-LDH concentration in the group 3 cohort was much higher than those of groups 1 and 2 ($P < 0.001$) (Fig. 1, A to C), implicating severer cytotoxicity with confounding condition. These differences were independent of age, gender, and total bilirubin of neonates (fig. S2, A to D).

To explore the relationship among CSF-LDH, blood pH, and direct bilirubin (DB), we performed the Spearman correlation analyses of all data from the three groups and found no correlation between blood pH and DB (fig. S2E). CSF-LDH did not show a strong association with variations in DB concentration or pH (group 1: $\rho = 0.152$, $P = 0.480$;

group 2: $\rho = 0.096$, $P = 0.364$) but became highly correlated with DB concentration over a broad concentration range (>10-fold differences) when concurrent acidosis occurred (group 3) ($\rho = 0.542$, $P < 0.001$) (Fig. 1D). CSF-LDH was strongly correlated with subtle decline in blood pH values in group 3 neonates confounded with hyperbilirubinemia ($\rho = -0.474$, $P < 0.001$). CSF-LDH was also correlated with acidosis (group 1: $\rho = 0.458$, $P = 0.024$) but not with hyperbilirubinemia alone (group 2: $\rho = 0.012$, $P = 0.913$) (Fig. 1F). Furthermore, the mean CSF-LDH concentration was higher in neonates with abnormal blood pH (133.2 ± 18.4 U/liter, $n = 71$) than in patients with normal blood pH (45.04 ± 1.44 U/liter, $n = 91$, $P < 0.001$) (Fig. 1, E and G). These results led us to postulate that bilirubin itself has limited toxicity but may exacerbate acidosis-dependent neuronal damage.

Bilirubin enhances ASIC currents in pH-dependent and voltage-independent manner

To interrogate the potential mechanisms underlying exacerbated neurotoxicity with confounding hyperbilirubinemia and acidosis, we examined whether there was an interaction between acid and bilirubin in the mouse MVN, one of the brainstem nuclei known to be particularly vulnerable to hyperbilirubinemia-associated toxicity. By making whole-cell recordings from acutely dissociated neonatal mouse MVN neurons, we found that protons (by switching solutions from pH 7.4 to 5.5) can evoke inward currents (I_{ASICs}) with pharmacological and biophysical characteristics typical of ASICs, as validated by their sensitivity and voltage-dependent block by tetraethylammonium (TEA)-Cl and BaCl₂ (fig. S3), which are known to block heterotrimeric ASICs (22). To test whether and how I_{ASICs} is modulated by bilirubin, we exposed MVN neurons to bilirubin at concentrations below the mean free bilirubin in CSF (14.51 ± 5.04 μ M/liter, $n = 14$; table S2) directly measured with the unagi fluorescent protein (UnaG)-based detection method (23). We found that I_{ASICs} was potentiated within 3 min of bilirubin application (9 μ M) during repeated presentation of acid ($P = 0.002$, $n = 7$) (Fig. 2, A and B). The enlarged currents were attenuated by amiloride (100 μ M), a classical blocker for I_{ASICs} , and this effect was reversible after a complete washout of bilirubin ($P = 0.003$, $n = 7$) (Fig. 2, A and B).

To establish the dose dependence of bilirubin on I_{ASICs} , we presented a series of concentrations of bilirubin for 3 min to MVN neurons and found that a maximal potentiation was achieved at 12 μ M (Fig. 2C). Construction of the pH dose-response curves before and after the application of 9 μ M bilirubin in the same MVN neurons revealed that bilirubin produced a relative larger potentiation of I_{ASICs} at lower pH than at higher pH, resulting in an apparent shift of the pH dose-response curve (pH_{50} : 5.56 ± 0.02 in control versus pH_{50} : 6.11 ± 0.02 after bilirubin; $n = 5$, $P < 0.001$) (Fig. 2D). This potentiation of I_{ASICs} appeared to be independent of the membrane potential or permeability of ASICs because bilirubin potentiated I_{ASICs} to a relatively similar extent at all potentials ranging from -60 to $+60$ mV, whereas the reversal potential remained the same (Fig. 2E). Collectively, these findings indicated that bilirubin makes ASICs more sensitive to protons and enhances their chord conductance, accounting for the increased amplitude of I_{ASICs} in MVN neurons. The maximal current density remained the same (Ctrl, control: 0.21 ± 0.09 nA/pF; Bil, bilirubin: 0.22 ± 0.1 nA/pF, $P = 0.447$), suggesting bilirubin mainly modulated the gating of ASICs without affecting the total number of channels on the membrane. Additional experiments demonstrated that bilirubin slowed the desensitization of ASICs (the decay time of I_{ASICs} activated at pH 5.5

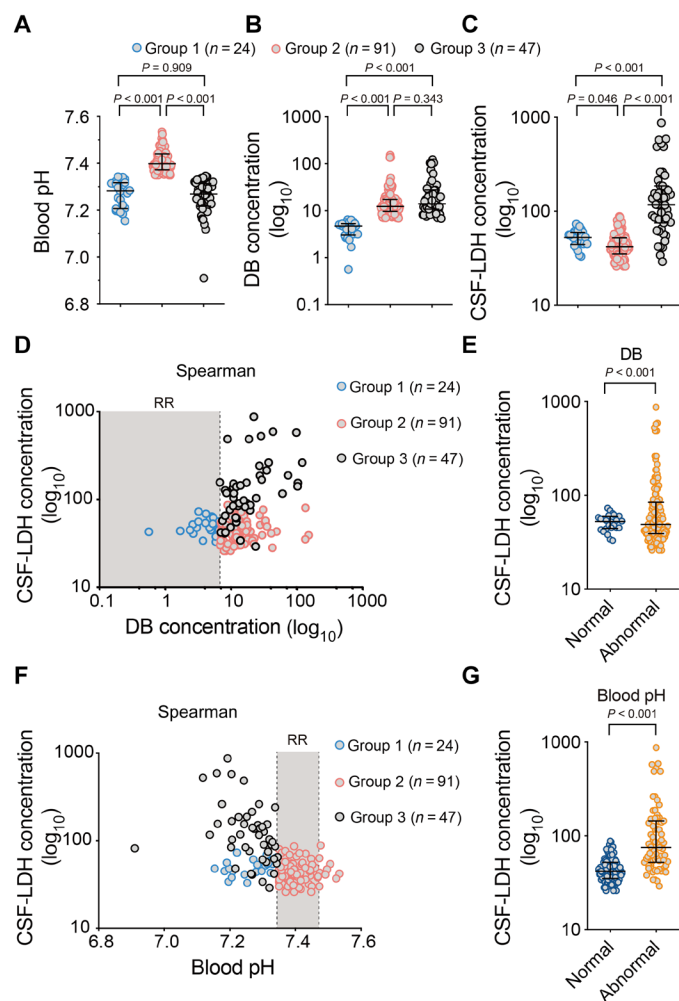


Fig. 1. CSF-LDH is correlated with blood pH and DB in neonates with hyperbilirubinemia and acidosis. (A to C) Data plots comparing blood pH, DB, and CSF-LDH in groups 1 ($n = 24$), 2 ($n = 91$), and 3 ($n = 47$) infants on the basis of reference range. Dunnett T3 test. (D) Scatter plots showing a correlation of CSF-LDH and DB in groups 1 to 3, Spearman correlation. RR, reference range. (E) Data plots comparing CSF-LDH in neonates with normal and abnormal DB. (F) Scatter plots by Spearman correlation analysis showing relationships of the CSF-LDH and blood pH in groups 1 to 3. (G) Data plots comparing CSF-LDH in neonates with normal and abnormal blood pH. Horizontal black lines represent median with interquartile range.

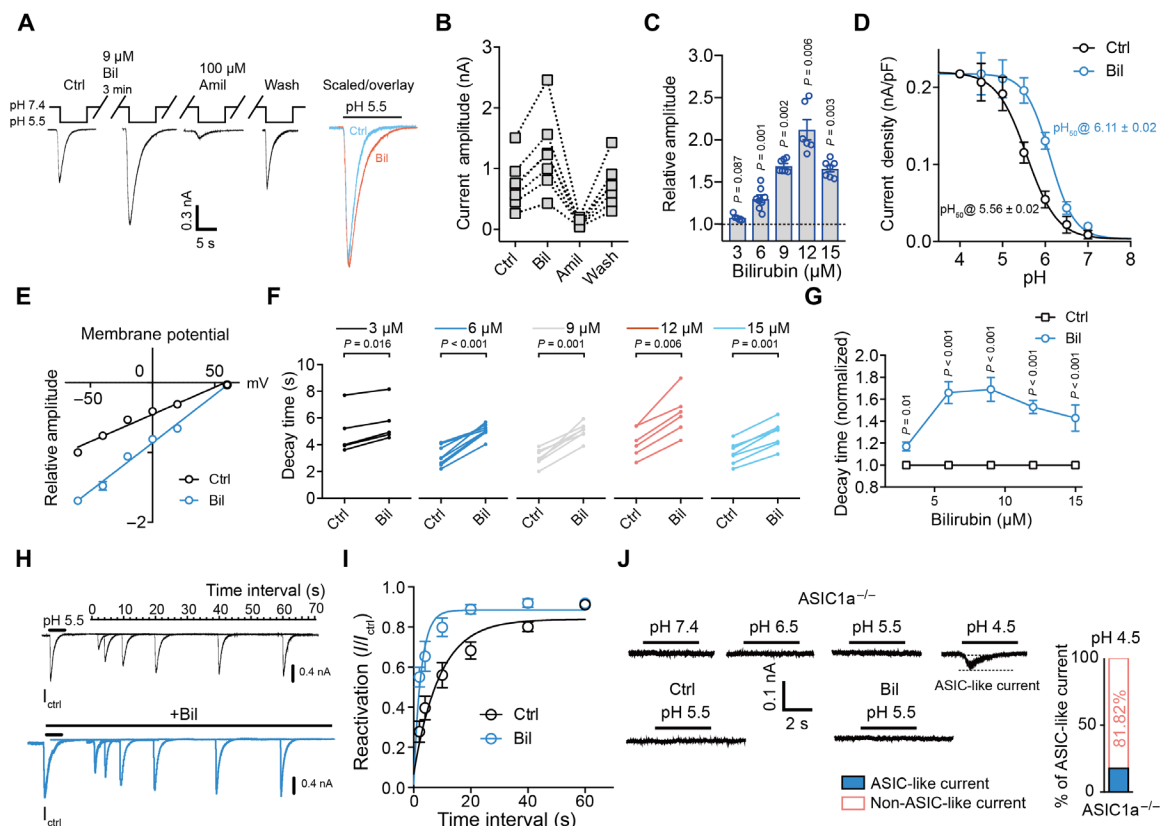


Fig. 2. Bilirubin directly potentiates I_{ASICs} . (A and B) Representative traces and summary data ($n = 7$) showing I_{ASICs} is potentiated by treatment of 9 μ M bilirubin and blocked by amiloride. Inset: Scaled and superimposed traces showing increase in the decay time course of I_{ASICs} before (blue) and after bilirubin treatment (red). (C) Summary data ($n = 5$ to 7) showing concentration-dependent potentiation of the I_{ASICs} in MVN neurons by bath application of bilirubin. (D) Fitted curves showing the pH dose-response curve for the ASICs with and without bilirubin. (E) Current-Voltage (I - V) curves were fitted by a straight line in the absence and presence of bilirubin with both reversal potentials at about +60 mV ($n = 5$). (F) Summary data showing the changes of decay time from the peak to baseline in different concentrations of bilirubin ($n = 5$ to 8). (G) Line chart showing the changes of normalized decay time in different concentrations of bilirubin. (H and I) Representative current traces and pooled data comparing recovery time courses from desensitization of I_{ASICs} before and after bilirubin (9 μ M) treatment, which was measured with double-pulse exposures to low-pH solution at different intervals (2 to 60 s). I_{ASICs} were activated by pH drop from 7.4 to 5.5. For each cell, the amplitude ratios of the second and the first I_{ASICs} were plotted as a function of time intervals, and the data are fitted with a single exponential function to yield time constants for recovery, $n = 5$ to 13. (J) Representative traces (left) showing activation of the I_{ASICs} in the absence and presence of bilirubin in *ASIC1a*^{-/-} mice. A weak ASIC-like current was recorded at pH 4.5 in a small number of *ASIC1a*^{-/-} cells (4 of 22 cells), as plotted in the right panel. Error bars represent means \pm SEM; Student's t test.

increased from 3.05 ± 0.24 s to 5.02 ± 0.24 s at 9 μ M, $n = 7$, $P = 0.001$) and accelerated their recovery from desensitization (Ctrl: $\tau = 9.121 \pm 1.332$ s, Bil: $\tau = 2.563 \pm 0.578$ s, $P = 0.005$; single exponential fits), again indicating its action on the gating of ASICs in MVN neurons (Fig. 2, F to I). Recordings of pH-activated currents with bilirubin in ASIC1a null neurons independently corroborated that ASICs are the sources of pH-dependent inward currents (Fig. 2J).

Ca²⁺-dependent signaling is involved in the potentiation of ASICs by bilirubin

Direct application of bilirubin did not evoke any current from MVN neurons, and its brief coapplication with acid did not enlarge I_{ASICs} , indicating bilirubin is neither an agonist (fig. S4, A and B) nor an allosteric modulator of ASICs (fig. S4, C and D). Instead, its potentiating effects on I_{ASICs} required several minutes to emerge (fig. S4E), implying that bilirubin must act through indirect intracellular signaling pathways. Considering that bilirubin is known to chelate zinc (24), which is known to have marked effects on the amplitude and properties of ASICs (25), we examined the effect of TPEN [*N,N,N',N'*-tetrakis(2-pyridylmethyl)

ethylenediamine] (10 μ M), a high-affinity chelator of zinc. Although zinc potentiated the ASIC currents, it did not occlude bilirubin-induced enhancement (fig. S4, F and G). In addition, given that bilirubin is thought to be easily oxidized, we tested the effect of biliverdin, its oxidative product, on I_{ASICs} and found no effect ($P = 0.929$) (fig. S4H). These results implicate a cross-talk between bilirubin and ASICs.

Given that bilirubin can readily permeate the membrane and modulate neuronal activities through intracellular Ca²⁺ ([Ca²⁺]_i)-dependent pathways (26), we examined whether [Ca²⁺]_i is required for bilirubin to potentiate the I_{ASICs} . We tested the effects of two Ca²⁺ chelators, ethylene glycol-bis(β -aminoethyl ether)-*N,N,N',N'*-tetraacetic acid (EGTA) and 1,2-bis-(2-aminophenoxyethane)-*N,N,N',N'*-tetraacetic acid (BAPTA). Each buffer was added respectively in the pipette solution to chelate [Ca²⁺]_i before testing the effect of bilirubin (Fig. 3A). Intracellular chelation of [Ca²⁺]_i with 20 mM BAPTA attenuated the bilirubin-induced enhancement of I_{ASICs} ($P < 0.001$); in contrast, 11 mM EGTA did not have an effect ($P = 0.879$) (Fig. 3, B and C). Knowing that the forward binding rate of BAPTA

is approximately 100-fold faster compared with EGTA despite similar equilibrium dissociation constant (27), we interpreted different effects of these two buffers as such that bilirubin-induced enhancement of I_{ASICs} requires a rise in $[Ca^{2+}]_i$, which is spatiotemporally tight-coupled to the downstream signaling pathways to up-regulate I_{ASICs} .

The blocking effect of BAPTA on the enhancement of I_{ASICs} by bilirubin suggested an involvement of Ca^{2+} -dependent intracellular signaling pathways such as protein kinases. To this end, we tested inhibitors for calmodulin-dependent protein kinase II (CaMKII) (Fig. 3D), which is known to be involved in mediating the intracellular effects of bilirubin (28). Addition of 5 μ M KN-93, an inhibitor of CaMKII, attenuated the enhancement of I_{ASICs} ($P < 0.001$) (Fig. 3E). Because CaMKII is associated with ASIC1a and enhances its activity by phosphorylation in other central neurons (28), we next examined whether bilirubin affects their physical interaction. Using immunoprecipitation and immunoblot analyses with antibodies against CaMKII and ASIC1a (Fig. 3F), we found that bilirubin increased the intensity of the CaMKII-specific band in ASIC1a pull-down after 1 hour of incubation, indicating that bilirubin promotes the association between ASIC1a and CaMKII (Fig. 3G). Together, these results suggested that CaMKII-dependent phosphorylation of ASICs (or their accessory proteins) is likely responsible for the Ca^{2+} -dependent up-regulation of I_{ASICs} by bilirubin in MVN neurons.

Bilirubin and acid produces synergistic effects on neuronal excitability

Activation of ASICs has been reported to cause membrane depolarization in hippocampal and retinal ganglion neurons (29, 30) and spike firings

(31), resulting in excessive Ca^{2+} inflow via themselves or other ion channels such as voltage-gated calcium channels (VGCCs). To directly test the functional impact of bilirubin-dependent potentiation of I_{ASICs} on neuronal excitability, we performed current-clamp recordings to examine the effects induced by ASICs activation with or without bilirubin exposure in MVN neurons (fig. S5, A to C). When we tested solutions with pH values ranging from pH 7.4 to 6.5–7.0, bilirubin was found to increase firing frequency, but a moderate decrease to pH 7.0 appears to generate the most enhancement (1.11 ± 0.23 to 2.26 ± 0.44 Hz, $n = 8$, $P = 0.002$) (Fig. 4, A and B), whereas more acidified solutions would lead to depolarization arrest of spiking.

Because both hyperbilirubinemia and acidosis were chronic pathological conditions, we next examined whether prolonged exposure to either acidic solution or bilirubin would affect the membrane excitability and spike firings. In the same MVN neuron, a brief 4-s drop in pH (from 7.4 to 7.0) triggered spike discharge, which immediately stopped upon switching back to normal saline. In contrast, a 2-min perfusion of extracellular pH 7.0 solution induced increased spike firing with a sustained membrane depolarization and continual spike firing even after switching back to the pH 7.4 solution, suggesting the increase in the excitability of MVN neurons can be long-lasting (Fig. 4C, left top). Although bilirubin alone did not produce a membrane depolarization, it markedly augmented the firing rate during and after 2 min of exposure to pH 7.0 solution (Fig. 4C, left bottom). In contrast, such changes were not observed in *Asic1a*^{-/-} neurons (Fig. 4, C, right and D). We noted a slight but persistent depolarization followed by bilirubin in both wild-type (WT) and *Asic1a*^{-/-} neurons after switching back to pH 7.4 (Fig. 4E),

Downloaded from <http://stm.sciencemag.org/> at Shanghai Jiaotong University on February 18, 2020

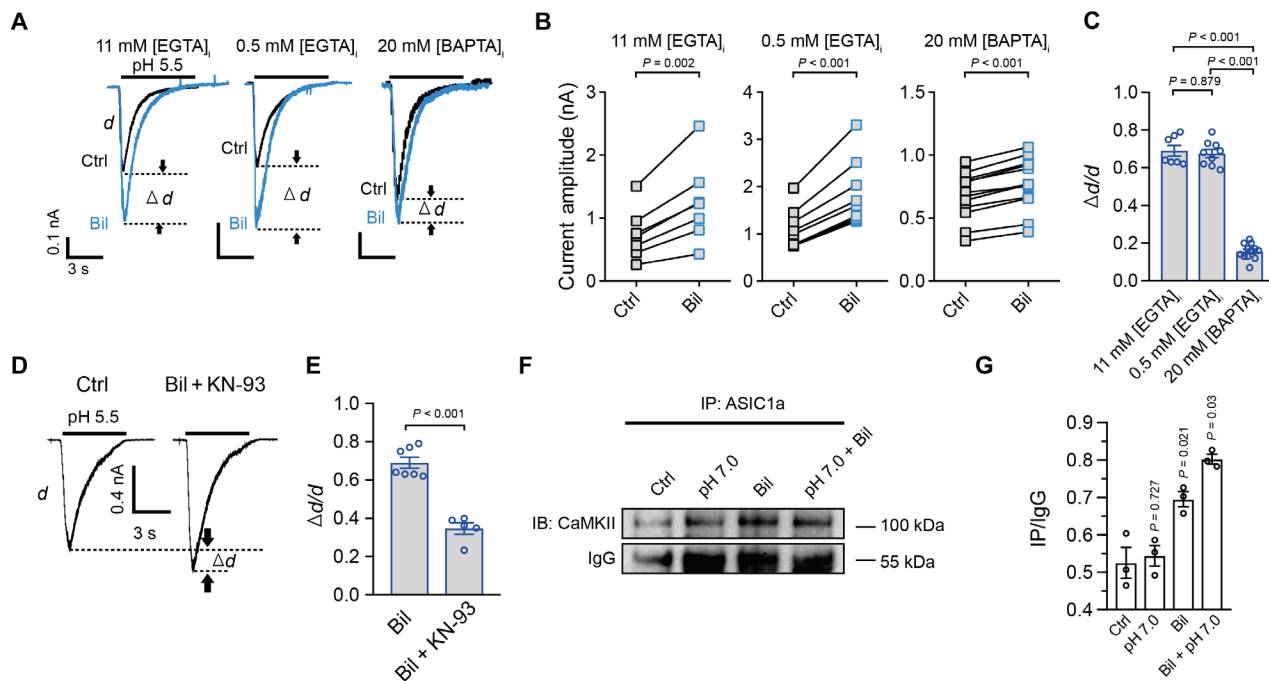


Fig. 3. Intracellular Ca^{2+} rise is engaged in bilirubin-induced potentiation of I_{ASICs} . (A) Representative traces showing bilirubin potentiation of I_{ASICs} in the presence of different Ca^{2+} -chelating agents, 11 mM EGTA ($n = 7$), 0.5 mM EGTA ($n = 9$), and 20 mM BAPTA ($n = 12$), which was respectively loaded into pipette solution. (B and C) Summary data showing the effect of 11 mM EGTA ($n = 7$), 0.5 mM EGTA ($n = 9$), and 20 mM BAPTA ($n = 12$) loaded in pipette solution on I_{ASICs} . (D) Representative traces showing the effect of KN-93, a blocker of CaMKII, on bilirubin-induced potentiation of I_{ASICs} . (E) Summary data showing the effects of bilirubin on I_{ASICs} in the presence and absence of KN-93. (F) Representative immunoblot (IB) analysis of CaMKII after immunoprecipitation (IP) of ASIC1a from brain tissues under different conditions. IgG, immunoglobulin G. (G) Analysis of coimmunoprecipitation (Co-IP) for CaMKII under the treatment of acidosis and/or bilirubin ($n = 3$ for each group). Error bars represent means \pm SEM; unpaired Student's t test and one-way ANOVA with post hoc Tukey's test.

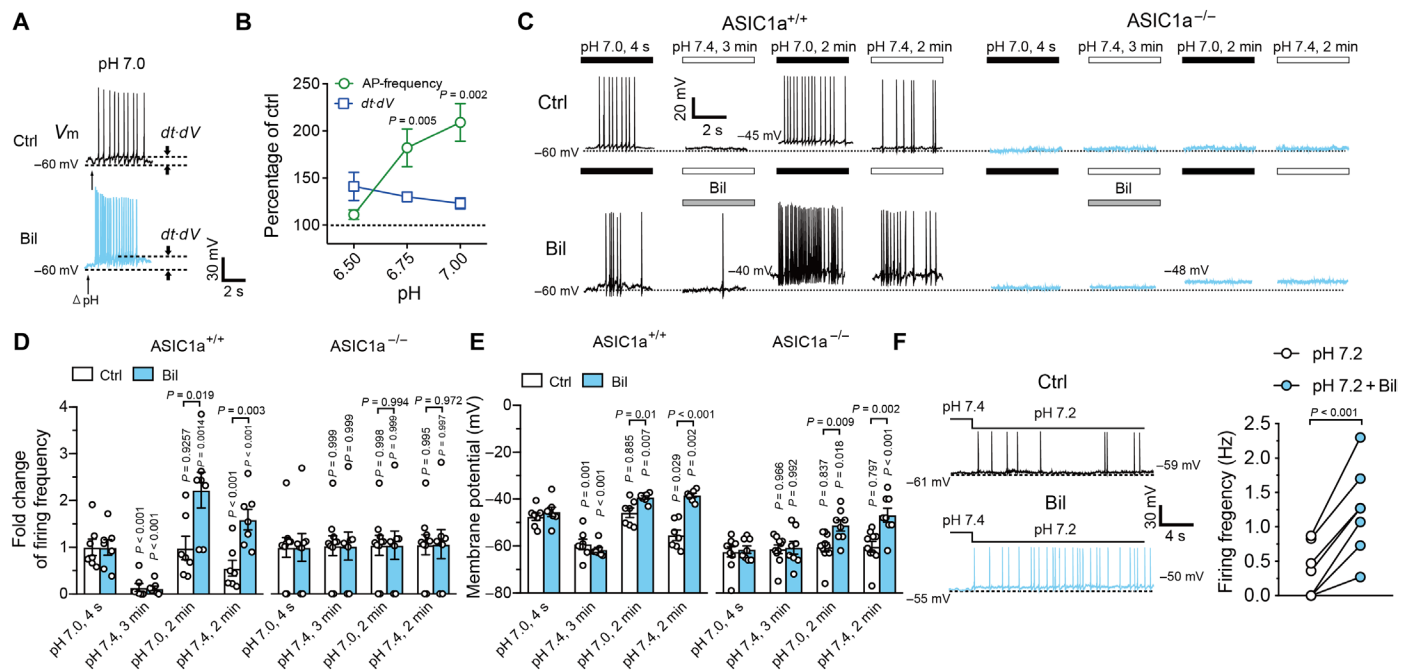


Fig. 4. Sustained membrane depolarization and firings by prolonged exposure to low pH and bilirubin. (A) Spike firings were recorded in current-clamp mode after pH drops from pH 7.4 to 7.0 in the absence and presence of 9 μ M bilirubin for 3 min. (B) Summary data showing the alteration of the firing frequency of evoked action potentials (AP) and the integral area of depolarization ($dt-dV$) induced by various pH drops with application of bilirubin ($n = 6$ to 8). (C) Representative traces showing the membrane potential and spike firings by a 4-s and 2-min pH drop from pH 7.4 to 7.0, followed by a 2-min washout before and after 9 μ M bilirubin in MVN neurons from WT ($n = 7$) and *Asic1a*^{-/-} mice ($n = 10$). (D) Summary data showing the firing frequency of action potentials in the absence and presence of 9 μ M bilirubin treatment for 3 min in neurons from WT and *Asic1a*^{-/-} mice ($n = 7$ to 10). (E) Summary data showing the changes of membrane potential in the absence and presence of 9 μ M bilirubin treatment for 3 min in neurons from WT and *Asic1a*^{-/-} mice ($n = 7$ to 10). (F) Representative traces and summary data showing the effect of a sustained (2 min) exposure of pH 7.2 on firing spikes in the absence and presence of 9 μ M bilirubin treatment for 3 min ($n = 9$). Error bars represent means \pm SEM; Student's *t* test, one- and two-way ANOVA with post hoc Tukey's test.

implying that some other unidentified cation channels that exist in both genotypes can be activated by bilirubin to elevate the resting membrane potential by a few millivolts. To corroborate the effect of bilirubin on neuronal excitability at an even milder pH value more consistent with clinical data, we examined the actions of pH 7.2 solution and found that I_{ASICs} did not desensitize as seen with more acidic solutions and that bilirubin robustly potentiated the total integral area of I_{ASICs} ($P < 0.001$) and the firing frequency ($P < 0.001$) after perfusion of bilirubin for 3 min (fig. S5D and Fig. 4F). These results demonstrated that bilirubin can amplify acid-dependent neuronal excitability and firings, synergistically contributing to neuronal overexcitation during pathological acidosis and hyperbilirubinemia.

Bilirubin potentiates acid-evoked intracellular Ca^{2+} transients

Previous studies have reported that in the CNS, ASICs are expressed abundantly and mainly in the form of either homotrimeric ASIC1a, heterotrimeric ASIC1a/2a, or ASIC1a/2b (22, 32–34), whereas ASIC3-containing channels play an important role in the peripheral nervous system (35–38). To investigate which isoform is the main correlate of native ASICs in MVN neurons, we studied the sensitivity of I_{ASICs} to different pharmacological blockers. We found that Psalmotoxin-1 (PcTx-1), a blocker for homotrimeric ASIC1a and heterotrimeric ASIC1a/2b but not for heterotrimeric ASIC1a/2a channels (22), had little effect on I_{ASICs} in MVN neurons at a concentration (50 nM) that significantly attenuated currents mediated by ASIC1a expressed in

Chinese hamster ovary (CHO) cells ($P < 0.001$) (fig. S6, A to C), indicating native ASICs are unlikely composed of homotrimeric ASIC1a or heterotrimeric ASIC1a/2b. Compound 5b, a new specific blocker of ASICs (39), inhibited I_{ASICs} (fig. S6, A and B). These implicated ASIC1a/2a as the molecular substrate. We further tested the sensitivity of native I_{ASICs} to two other blockers, BaCl₂ and TEA-Cl, with the former being more effective in blocking heterotrimeric ASIC1a/2b than heterotrimeric ASIC1a/2a or homotrimeric ASIC1a, whereas the latter being less selective (22). We found that BaCl₂ had very little effect on I_{ASICs} in MVN neurons, but TEA-Cl produced a robust inhibition (10 mM TEA-Cl: $34.56 \pm 0.97\%$; 10 mM BaCl₂: $9.12 \pm 0.38\%$; $n = 5$ to 7, $P < 0.01$) (fig. S6, A and B). These results suggest that bilirubin potentiation of I_{ASICs} in MVN neurons is caused to a large extent by heterotrimeric ASIC1a/2a channels, as validated by our characterization of biophysical and pharmacological properties of I_{ASICs} in MVN neurons from WT mice (fig. S6, A to G). Last, we recapitulated bilirubin's effect on ASIC1a/2a expressed in CHO cells, consistent with that in WT neurons (fig. S6, H to J).

Knowing intracellular Ca^{2+} rise is involved in the potentiation of I_{ASICs} by bilirubin but native ASIC1a/2a channels are Ca^{2+} impermeable, we further explored the sources of Ca^{2+} rise and discerned the effects of bilirubin on acid-induced $[Ca^{2+}]_i$ elevation by using fluorescent Ca^{2+} imaging with fluo-3 AM. The reduction in extracellular pH from 7.4 to 7.0 induced a slight elevation of $[Ca^{2+}]_i$; an elevation of $[Ca^{2+}]_i$ was caused by a pH drop to 5.5, which was nearly abolished by the ASIC antagonist amiloride (fig. S5E). Consistent with previous

studies, bilirubin itself could cause small $[Ca^{2+}]_i$ elevation by a brief perfusion. The same exposure of bilirubin augmented the acid-induced $[Ca^{2+}]_i$ elevation in WT MVN neurons, and this effect was blocked in the *Asic1a*^{-/-} cells (Fig. 5A). After prolonged washout with pH 7.4 solution, the fluorescence intensity of $[Ca^{2+}]_i$ remained at a higher concentration in WT neurons compared with that in *Asic1a*^{-/-} neurons (Fig. 5, B and C). Comparison of the integral areas of Ca^{2+} responses indicates that the effects of bilirubin on acid-induced $[Ca^{2+}]_i$ elevation are ASIC dependent, long-lasting, and supralinear (Fig. 5, D and E). This result is consistent with the observation that bilirubin prolonged the opening of ASICs to increase neuronal excitability, resulting in an overload of $[Ca^{2+}]_i$ and, consequently, neurotoxicity.

To examine the source of supralinear rise in Ca^{2+} integrals during low pH and bilirubin, we tested the possible contribution of other Ca^{2+} -permeable channels. The action potentials evoked by low pH are known to facilitate the activity of VGCCs, which may result in the excessive influx of Ca^{2+} . Addition of $CdCl_2$ (200 μ M), a nonspecific blocker of VGCCs, into the bath solutions attenuated the $[Ca^{2+}]_i$

rise, suggesting that the acid-induced $[Ca^{2+}]_i$ elevation is largely caused by the compounded effects from intracellular Ca^{2+} release and influx via VGCCs during repetitive spike firings (Fig. 5F).

Bilirubin aggravates neurotoxic effects by potentiating the activity of ASICs

To directly test whether bilirubin works via ASICs to exacerbate cell death, we performed cell injury assays in MVN slices from WT and *Asic1a*^{-/-} mice by fluorescence staining of alive and dead cells (with basal cell death about ~40% likely due to acute brain slice preparations; fig. S7A). The mortality of MVN neurons from WT showed an increase at pH 7.0 compared to that at pH 7.4 ($P = 0.018$), whereas *Asic1a*^{-/-} mice at pH 7.0 showed no significant change ($P = 0.319$). In the presence of bilirubin, acidification enhanced neural death in WT ($P < 0.001$) but not in *Asic1a*^{-/-} slices ($P = 0.058$) (Fig. 6A). The mortality of MVN neurons was also reduced by 1 hour before incubation of BAPTA-AM ($P < 0.001$) (Fig. 6A) and compound 5b ($P < 0.001$) but not PcTX-1 ($P = 0.364$) compared with that in bilirubin at pH 7.0 (Fig. 6B). Given the previously reported cross-talk between ASIC1a

and *N*-methyl-D-aspartate receptors (NMDARs)–NR2B under ischemic conditions, we also performed cell death assays in the presence of MK801, a specific pore blocker of NMDARs. We found that MK801 attenuated mortality under bilirubin and acid conditions in WT ($P < 0.001$) but not in *Asic1a*^{-/-} neurons ($P = 0.557$) (Fig. 6C), implicating the dominant role of ASICs over NMDARs in mediating cell death under confounding hyperbilirubinemia and acidosis conditions, despite the fact that bilirubin can increase the association between ASIC1a and NR2B (fig. S7B). $CdCl_2$, a nonspecific inhibitor of VGCCs, was most effective in attenuating cell death ($P < 0.001$) (Fig. 6D), in line with the findings that bilirubin enhanced the activity of ASICs and firings to overload $[Ca^{2+}]_i$ in WT but not in *Asic1a*^{-/-} neurons. Similarly, bilirubin did not induce any cell death at pH 7.0 in nontransfected CHO cells (fig. S7C) but increased the mortality of ASIC1a/2a–green fluorescent protein (GFP)–transfected CHO cells ($P < 0.001$) (Fig. 6E). Together, these data strongly argue that ASIC1a-containing channels are the molecular substrate underpinning bilirubin-induced cell death after intracellular Ca^{2+} overload.

To consolidate the role of bilirubin in ASIC1a-induced neuronal injury, we measured the release of LDH from slices. Compared to slices treated at pH 7.4, exposure of slices for 1-hour to acidic solution at pH 7.0 or bilirubin containing solution at pH 7.4 increased LDH release. However, a stronger increase was induced by bilirubin at pH 7.0. Bilirubin was

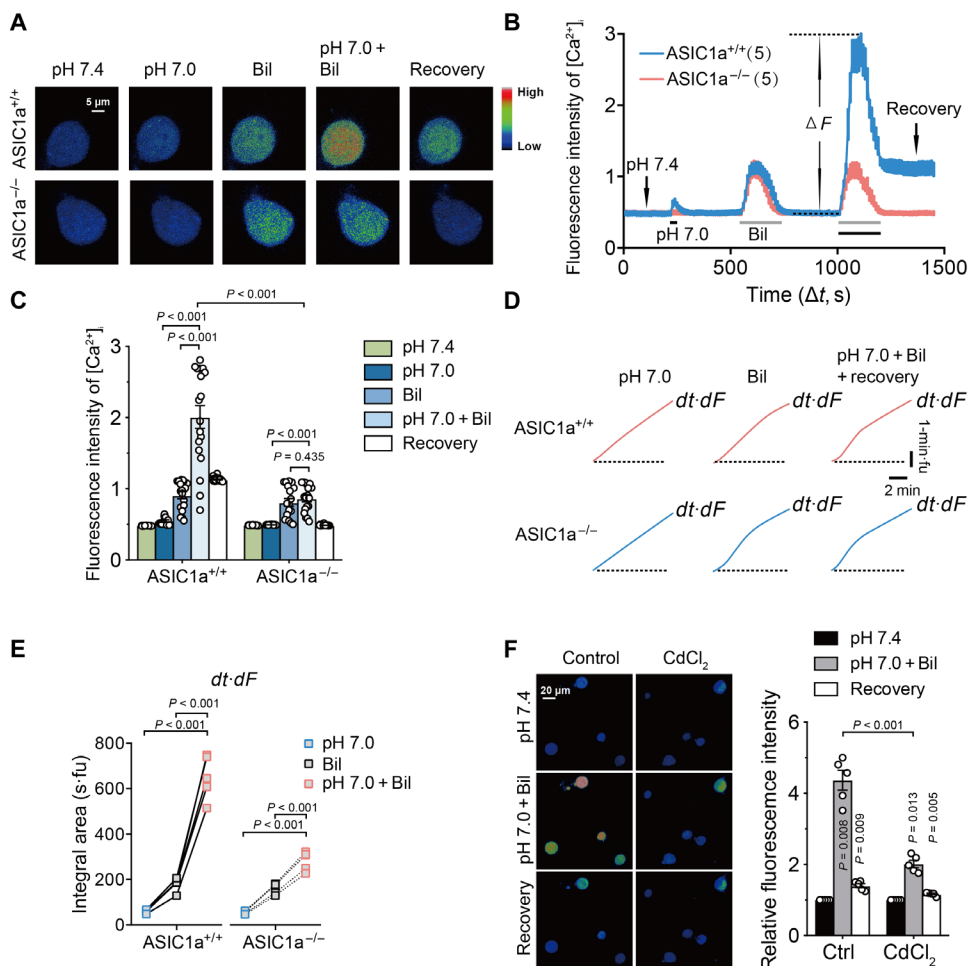


Fig. 5. Bilirubin enhances acid-induced elevation of $[Ca^{2+}]_i$ in neurons of MVN. (A and B) Example images and time courses of changes in fluorescence intensity of $[Ca^{2+}]_i$ evoked by a pH drop from 7.4 to 7.0 in the absence and presence of bilirubin in neurons from WT and *Asic1a*^{-/-} mice. (C to E) Summary data showing differences in the amplitude or integral area of fluorescence intensity of $[Ca^{2+}]_i$ in WT and *Asic1a*^{-/-} mice (fu, fluorescence intensity unit). The time window is 200 s for the integral area after the solution switch. (F) Representative images and pooled data showing the effect of 200 μ M $CdCl_2$ on supralinear increases in $[Ca^{2+}]_i$ by acid and bilirubin ($n = 5$). Error bars represent means \pm SEM; Student's *t* test, one- and two-way ANOVA with post hoc Tukey's test.

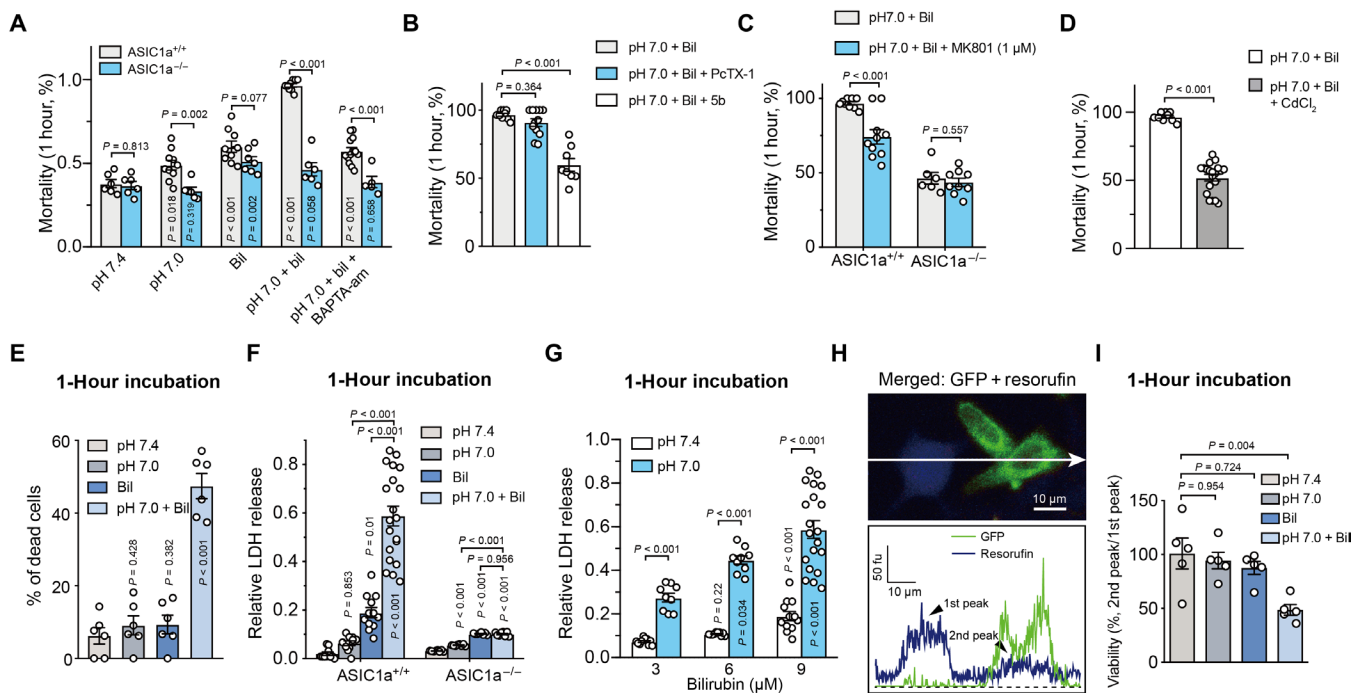


Fig. 6. Bilirubin enhanced acid-dependent cell death. (A) Summary data showing the mortality ratio of MVN neurons in WT and *Asic1a*^{-/-} mice respectively under different bath conditions for 1 hour (Bil: 9 μM; BAPTA-am: 50 μM) (*n* = 6 to 13). (B) Summary data showing the effect of two specific blockers of ASIC1a, PctX-1 (50 nM) and compound 5b (10 μM), on mortality with both bilirubin (9 μM) and acidosis (pH 7.0) (*n* = 8 to 12). (C) Summary data showing the effect of MK801 (1 μM), an inhibitor of NMDARs, on the mortality of MVN neurons in WT mice but not in *Asic1a*^{-/-} mice (*n* = 6 to 10). (D) Summary data showing the effect of CdCl₂ (200 μM), a nonspecific inhibitor of VGCCs, on the mortality of MVN neurons (*n* = 9 to 20). (E) Summary data showing the percentage of dead cells in ASIC1a/2a-GFP-transfected CHO cells at pH 7.0 in the treatment of bilirubin (*n* = 6). (F) Summary data showing the LDH release assay in slices from WT and *Asic1a*^{-/-} mice incubated in different conditions (*n* = 10 to 20). (G) Dose-dependent LDH release assay by incubation of bilirubin in pH 7.4 and 7.0 solution (*n* = 9 to 10). (H) Top: Representative image of nontransfected and ASIC1a/2a-GFP-transfected CHO after 1-hour incubation in bilirubin (9 μM) and pH 7.0 extracellular solution showing line scan position (white arrow). Bottom: Quantified fluorescence from GFP and resorufin (fu, fluorescence units). First and second peaks represent the maximal fluorescence of resorufin in two types of CHO cells. (I) Summary data showing the viability of ASIC1a/2a-GFP-transfected CHO cells in different conditions by normalizing their blue fluorescence intensity to those of nontransfected neighbor cells (percentage of second peak to first peak). (*n* = 5). Error bars represent means ± SEM; Student's *t* test, one- and two-way ANOVA with post hoc Tukey's test.

ineffective in potentiating cell injury in *Asic1a*^{-/-} neurons (Fig. 6F). The effect of bilirubin on LDH release was concentration dependent (Fig. 6G). The viability of CHO cells was further assessed by the cell titer blue assay, using resorufin as a fluorescent marker of live cells (Fig. 6H, color-coded dark blue). In ASIC1a/2a-GFP-transfected cells, bilirubin and acidosis alone failed to induce reduction in blue fluorescence intensity (fig. S7, D to F). Coapplication of bilirubin and pH 7.0 caused a reduction in blue fluorescence intensity (Fig. 6, H and I), demonstrating that bilirubin itself has subtle effects on cell viability but aggravates cell damage through ASIC1a-containing channels. Together, these results support a new functional link between hyperbilirubinemia and acidosis-mediated cell injury and death that might help to explain the clinical evidence showing a markedly higher CSF-LDH concentration in infants with concurrent hyperbilirubinemia and acidosis.

Concurrent hyperbilirubinemia and acidosis in mouse neonates cause long-term damage to brain functions

To model the effects of hyperbilirubinemia with or without concurrent acidosis in vivo, we subjected neonatal mice (P3) to three separate experimental conditions on a daily basis for 1 week: condition 1 [hyperbilirubinemia (HB)]: Mice were injected (intraperitoneally) with bilirubin (50 μg/g); condition 2 [acidosis (AS)]: Mice were placed

in a low-oxygen chamber (10% O₂) for 1 hour per day; and condition 3 (HB + AS): Mice underwent both bilirubin injections and low-O₂ exposure; these groups were compared with the vehicle (injected with phosphate-buffered saline buffer) group. At P10, we assessed the permeability of the BBB in vivo by injecting Evans Blue, an intravital blue dye that binds to albumin and penetrates into the brain only when BBB is compromised. As shown in Fig. 7A, we found that all the brain slices from the AS and AS + HB groups were stained blue (optical density, *P* < 0.001; Fig. 7B, left), especially in the hippocampus, brainstem, and cerebellum with minimal staining of the cortex (Fig. 7B, right). These results demonstrated that acidosis, but not hyperbilirubinemia, increased the permeability of BBB and that this effect is not dependent on ASICs because brain slices from *Asic1a*^{-/-} mice showed similar degrees of Evans Blue staining under the condition of concurrent AS + HB. To validate acidification of CSF after hypoxia, we tested the blood and CSF pH of AS mice immediately after hypoxia conditioning (fig. S8A). As shown in fig. S8B, we found that the CSF pH (7.188 ± 0.129) is higher than the blood pH (6.688 ± 0.067, *P* = 0.009), justifying our choices of solutions with different degrees of acidification for experiments in vitro. In addition, the exacerbated brain injury by HB + AS over either condition alone was independently validated by elevated CSF-LDH at P10 in a subset of neonatal mice (fig. S8, C to E). Age-dependent

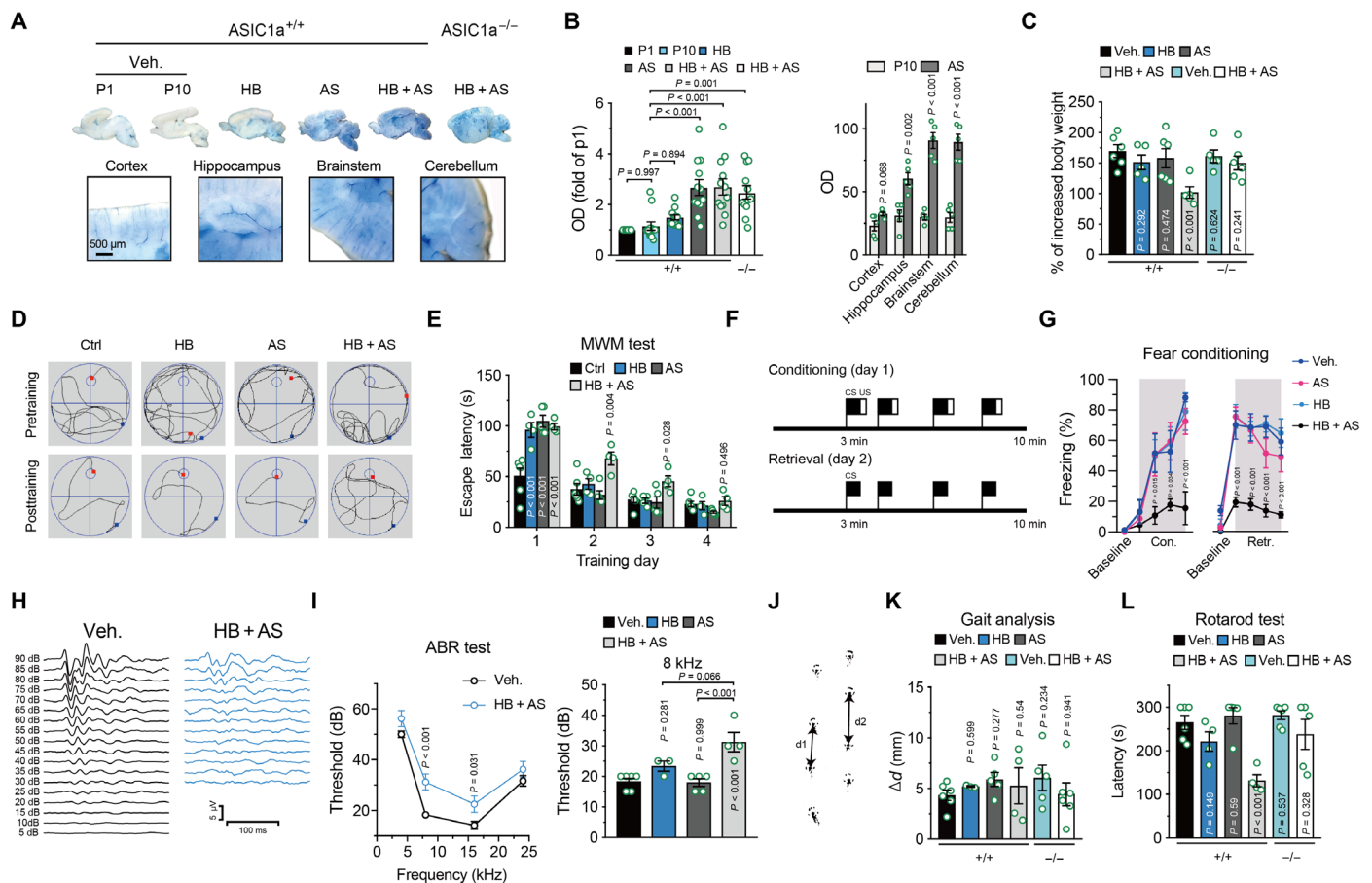


Fig. 7. Behavioral deficits in mouse models with early postnatal exposure to hyperbilirubinemia, acidosis, and both. (A) Representative images of dissected brain slices from mice from six different experimental conditions revealing permeability of BBB in global brain labeled by Evans Blue (top). Veh., vehicle at P1/P10; HB, hyperbilirubinemia; AS, acidosis; it should be noted that HB, AS, HB + AS in WT, and HB + AS in *AsiC1a*^{-/-} mice were all conditioned for 7 days before Evans Blue were injected at the age of P10. Zoom-in images of cortex, hippocampus, brainstem, and cerebellum dyed by Evans Blue (bottom). (B) Summary data showing the global optical density (OD) of Evans Blue for slices from different groups (left, *n* = 12) and regional OD of cortex, hippocampus, brainstem, and cerebellum between Veh. and AS mice at P10 (right, *n* = 5). (C) Summary data showing the percentage of age-dependent increase in body weight between P10 and P3 under different conditions (*n* = 5 to 6). (D) Representative real-time track records of mice in MWM test. The smaller blue circle represents the platform, the blue and red points represent the starting and stopping position, respectively. (E) Summary data showing the escape latency for mice to find the platform in the MWM test (*n* = 4 to 6). (F) Experimental scheme for the fear conditioning test: The mice were placed in the chamber for 3 min to test the initial fear time (baseline freezing in percentage) before pairing pure tone (CS, 4 kHz, 76 dB, 30 s) and foot shock (US, 0.5 mA, 2 s). (G) Summary of freezing time during fear conditioning (Con., left) and retrieval (Retr., right). One-way ANOVA with post hoc Tukey's test was used to compare the differences among animal groups in each trial (Veh., *n* = 6; AS, *n* = 6; HB, *n* = 4; HB + AS, *n* = 6). (H) Representative traces showing the typical ABR waveforms from the Veh. and HB + AS groups mice at the testing frequency of 8 kHz. (I) Line chart (left) showing the thresholds of Veh. mice and HB + AS models at frequencies of 4, 8, 16, and 24 kHz in ABR recordings, and bar graph (right) showing that the threshold of the HB + AS group mice was higher than that of the other groups at the frequency of 8 kHz (*n* = 3 to 6). (J) Representative image showing the footprints from the Veh. group, d1 and d2, respectively, represent the left and right stride length measured along a line connecting two consecutive prints from the same paw. (K) Summary data showing the difference between the right and left stride length among the different groups (*n* = 3 to 6). (L) Summary plot showing the time for mice to fall off the rod (*n* = 4 to 6). It should be noted that *AsiC1a*^{-/-} mice are well known for their major behavioral deficits, for example, in learning and memory (13), and were, thus, not subjected to all tests in parallel. Error bars represent means ± SEM; unpaired Student's *t* test and one-way ANOVA with post hoc Tukey's test.

increase in body weight in HB + AS mice was markedly lower than that in the other two groups models and even in HB + AS *AsiC1a*^{-/-} mice (*P* < 0.001) (Fig. 7C), implicating a globally negative impact of concurrent hyperbilirubinemia and acidosis on development.

Previous clinical studies have reported that neurodevelopment impairments by kernicterus may occur during the first year of life, such as low weight at birth, learning disability, movement disorders, and sensorineural hearing loss (11). To examine the long-term impact of early neonatal conditioning on brain functions, we designed a series of behavior experiments for three groups of WT mice when

they reach the age of 4 to 5 weeks after 7 days of conditioning from P3 to P10. To test hippocampus-based functions, we performed the Morris water maze (MWM) test (Fig. 7D) and found that all mice with HB, AS, or HB + AS conditioning showed longer delays to find the hidden platform than those without conditioning. Although all mice were able to learn and remember the task over 4 days of training by requiring less time to reach the platform, HB + AS mice showed consistent deficits in completing the task (Fig. 7E). Considering that HB + AS mice may have motor deficits that affect their performance in MWM, we conducted the fear conditioning test, which represents

a contextual learning and memory paradigm that is dependent on the hippocampus but not brain regions for motor coordination (Fig. 7F). We found that HB + AS mice exhibited much lower freezing response to tone as conditional stimuli (CS) during fear conditioning ($F_{3,18} = 14.46$, $P < 0.001$ in the fourth CS) and retrieval compared with the other two groups of mice ($F_{3,18} = 8.81$, $P < 0.001$ in the fourth CS; Fig. 7G). These results implicated that HB + AS conditioning during the early neonatal stage can lead to prominent spatial learning and memory abnormalities later on. Given the prominent extravasation of Evans Blue into the hindbrain after HB, AS, and HB + AS conditioning, we further examined the sensorimotor functions of the three groups of conditioned mice. By measuring and comparing the auditory brainstem responses (ABRs), we found that HB + AS WT mice showed an upward shift in threshold at all frequencies, with 8 kHz being the most affected ($P < 0.001$) (Fig. 7, H and I). Gait analysis using stride length measurements showed that all mice were able to control their basic balance and motor functions (Fig. 7, J and K). However, when we challenge these mice with accelerating the rotarod, we found that HB + AS WT mice, but not HB or AS mice, displayed a deficit in staying on the rod as evidenced by 50% decrease in the latency to fall (Fig. 7L). This deficit was completely absent in *Asic1a*^{-/-} mice. These results suggested that early conditioning of neonatal brains with HB + AS can work through ASICs to negatively affect the long-term trajectory of both sensory and cognitive functions of the developing brain.

DISCUSSION

Bilirubin-induced neurotoxicity is widely accepted as a leading cause of hearing loss, balance, motor control, and cognition deficits in children with severe clinical hyperbilirubinemia, and is often aggravated by confounding factors such as prematurity, infection, sepsis, hypoxia, ischemia, and acidosis (11, 21), all of which may increase the permeability of BBB to bilirubin. It is classically believed that acidosis promotes precipitation of bilirubin in the developing brain where differentiating neurons are vulnerable to bilirubin toxicity (40–43). Our analyses of clinical data from three populations of neonates demonstrated that coexistence of hyperbilirubinemia and acidosis leads to more severe brain injury, as indicated by CSF-LDH, than either condition alone. However, the steep dependence of CSF-LDH on pH but not DB (over a wide range of concentration: 10 to 100 $\mu\text{M}/\text{liter}$) prompted us to investigate the possibility that bilirubin enhances ASIC-dependent neurotoxicity. DB is one of the major forms of bilirubin in blood detectable in clinical (direct, indirect, conjugated, and unconjugated) and is thought to be positively correlated to the free bilirubin concentration and neurotoxicity (44). Notably, the pathologically relevant concentrations of free bilirubin remain elusive and debated, in part due to the challenge that clinical biochemical measurements of peak bilirubin often mismatch the appearance of symptoms in human neonates. However, previous studies from a widely accepted model, the Gunn rat model, showed that free bilirubin was 2743 to 10080 nM (45, 46). Our pilot study indicated that free bilirubin concentrations in the CSF of neonates with hyperbilirubinemia also fall into a similar micromolar range, supporting the idea that the bilirubin concentrations used in the experiments are clinically relevant. Our experiments in vitro with relevant bilirubin concentrations showed it has marginal effects on neurotoxicity but enhances ASIC activity in MVN neurons and their overexcitation, $[\text{Ca}^{2+}]_i$ overload, and cell death (LDH release). Bilirubin's effects appear to be the most robust for moderate decreases

in pH, 7.0 to 7.3, which are consistent with previously reported CSF pH values in neonates with acidosis (47). Our findings implicate the necessity of carefully monitoring the pH for the clinical management of hyperbilirubinemia.

Clinical indicators such as brainstem auditory evoked potentials or ABRs help establish the predictive validity in determining the specific sites of bilirubin-induced brain damage (1, 42, 48); however, absence of gross degenerative changes in the auditory brainstem suggests that subcellular or biochemical factors should be sought to reflect the early neuropathological changes in neonatal hyperbilirubinemia. Our clinical datasets indicate that CSF-LDH is increased in neonates undergoing hyperbilirubinemia, acidosis, or both. This suggests that CSF-LDH is a reliable and objective index of tissue breakdown, particularly for brain damage, and that comparison of the measured LDH values and pH changes for children experiencing clinical hyperbilirubinemia may help guide not only diagnosis but also treatment (49, 50). This is in line with assays for which the LDH concentration is widely used in basic studies for cell injury assay (20, 51, 52). It should be noted that these assays focus on chronic effects of hyperbilirubinemia and acidosis with incubation time being 1 hour, which differ from our electrophysiology experiments that use acute treatment for 3 min. The relative LDH release was markedly increased in neonatal mouse brain slices incubated in bilirubin at pH 7.0 or CSF of neonatal mice conditioned with HB and AS, consistent with the clinical observations mentioned above.

Our extensive biophysical and pharmacological analyses of bilirubin's effects on the neonatal mouse MVN neurons indicate that native ASICs are likely heterotrimeric, composed of ASIC1a and ASIC2a subunits. Homotrimeric ASIC1a and heterotrimeric ASIC1a/2a and ASIC1a/2b are the most abundant ASIC configurations in CNS neurons (53, 54), and their pharmacological properties depend on the subunit composition. Heteromeric ASIC2a and 2b have been shown to be relatively insensitive to protons (17). Unlike homotrimeric ASIC1a, which is permeable to Ca^{2+} and sensitive to PcTX-1, ASIC1a/2a and ASIC1a/2b are sensitive to TEA-Cl and barium, with ASIC1a/2a being less sensitive to barium than ASIC1a/2b. Moreover, the inhibition of ASIC1a/2a and ASIC1a/2b by TEA-Cl and barium exhibits different voltage-dependent relationships (22). Our findings that BaCl_2 has a weak inhibitory effect on the bilirubin-induced potentiation of I_{ASICs} and that small pH drop does not appear to increase $[\text{Ca}^{2+}]_i$, implicate ASIC1a/2a as the main molecular correlate of I_{ASICs} without Ca^{2+} permeability in native MVN neurons. Our observations that compound 5b, a new blocker for ASIC1a homomeric and ASIC1a/2a heteromeric channels, effectively blocks native ASIC currents, which are insensitive to PcTX-1, a specific blocker for homomeric ASIC1a and heteromeric ASIC1a/2b (22), lending further support to the postulate that ASIC1a/2a channels are the most likely correlate of native ASICs in MVN neurons. Pharmacological titration of ASIC currents with compound 5b by 50% was sufficient to attenuate cell death, whereas genetic knockout of ASIC1a ablates the native I_{ASICs} from MVN and cell death reinforces our view that bilirubin-dependent enhancement of ASICs accounts for aggravated cell death under hyperbilirubinemia and acidosis. Moreover, ASIC1a/2a has a low H^+ sensitivity with the half-maximal activation at pH 5.4 to 6.1 (55), in line with what we have observed for bilirubin-induced potentiation of I_{ASICs} being pH dependent. These collectively support the argument that heterotrimeric ASIC1a/2a is the primary form of ASICs in MVN neurons.

Bilirubin can increase neuronal excitability and spontaneous firings in developing neurons, possibly allowing Ca^{2+} influx via VGCCs as

well as intracellular Ca^{2+} release from internal stores (56–59). The elevated $[\text{Ca}^{2+}]_i$ in turn increases CaMKII-dependent phosphorylation of ASICs and potentiates the amplitude of I_{ASICs} (60, 61). In line with findings by Gao *et al.* (19) that ASICs are physically associated with CaMKII to promote protein phosphorylation including ASICs themselves, we demonstrated that bilirubin can increase the association between ASIC1a and CaMKII. CaMKII can be activated by Ca^{2+} binding to CaM and involved in bilirubin-induced neuronal toxicity (62); thus, the findings that the enhanced ASIC activation was abolished by BAPTA loaded into neurons to chelate $[\text{Ca}^{2+}]_i$ and that neuronal mortality was decreased by BAPTA or CdCl_2 suggest that Ca^{2+} plays a critical role in activating intracellular signaling cascades to potentiate I_{ASICs} . In addition, membrane depolarization induced by ASIC1a-containing channels and glutamate or GABA_A receptors also contributes to the activation of VGCCs, leading to $[\text{Ca}^{2+}]_i$ overload and, thus, cell death (59, 63, 64). We conceptualize our findings from these *in vitro* experiments that bilirubin potentiates ASIC activity via Ca^{2+} -dependent signaling and overload, ultimately resulting in cell injury and death in neonatal brains.

Our findings *in vitro* led us to test the hypothesis that neonatal hyperbilirubinemia concurrent with acidosis may cause long-term brain damage *in vivo*. Neonatal mice with acidosis through hypoxia exhibit an increase in BBB permeability, confirming that acids enhance the accessibility of bilirubin to the brain, where it precipitates to exert its neurotoxicity. However, the concentration of bilirubin alone does not predict the risk of encephalopathy, as bilirubin-induced neurotoxicity depends on complex interactions between its concentration and the cellular characteristics of the developing brain as demonstrated in this study and inferred by others (21). Behavioral experiments in this study showed that neonatal mice with early HB + AS conditioning exhibited more profound deficits in spatial memory, sensorimotor function, and hearing than either HB or AS alone when they reach adulthood. Because these tasks depend on the hippocampus, cerebellum, and brainstem, including vestibular and auditory nuclei where ASIC1a is expressed abundantly and bilirubin seems to preferentially precipitate (65), our observations, thus, corroborate the idea that bilirubin and ASIC1a play a synergistic role in causing early brain damage that can be manifested as profound long-term neurological phenotypes later in life.

The study presents some limitations: The ethical issues for us to timely access infant CSF samples in the intensive care unit (ICU) have precluded us from testing the pH of brain fluid from clinical subjects with hyperbilirubinemia and/or acidosis. As a result, we only have blood pH values of these subjects as a proxy for correlation analyses of clinical datasets. It is still unclear whether the CSF pH values in those patients are consistent with those in our mouse models *in vitro* and *in vivo*. Furthermore, long-term neurological and cognitive outcomes in subjects with hyperbilirubinemia and/or acidosis are rather heterogeneous. Neonates with hyperbilirubinemia and acidosis will usually receive immediate treatments including phototherapy (66) and correction of respiratory acidosis to raise the brain pH (42). Despite these effective interventions, some neonates still develop lifetime impairments in sensorimotor and cognitive functions. Future studies are clearly needed to address why and how neonatal hyperbilirubinemia can lead to irreversible neurotoxicity in a subset of subjects. This study exemplifies acidosis as one of the risk factors of other medical conditions along with hyperbilirubinemia.

In conclusion, our findings from clinical subjects with hyperbilirubinemia and/or acidosis and experiments on mouse neonatal

neurons *in vitro* converge onto the idea that their synergistic actions are largely mediated by effects of bilirubin on ASIC1a-containing channels. These channels can boost the neuronal excitability and $[\text{Ca}^{2+}]_i$ overload via VGCCs and Ca^{2+} release beyond the capacity of neonatal neurons to cope, ultimately leading to neuronal injury and long-term sensory and cognitive impairments *in vivo*. We advocate that protecting neurons from excitotoxic insults requires serious attention to CSF-LDH and pH in clinical hyperbilirubinemia including those with genetic risks (5, 6) and that ASIC1a be considered as a potential target for the treatment of confounding hyperbilirubinemia and acidosis, hypoxia, and ischemia in infants.

MATERIALS AND METHODS

Study design

We designed this study to investigate the quantitative relationships between acidosis, hyperbilirubinemia, or both conditions with the extent of brain injury in newborns experiencing severe hyperbilirubinemia in the ICU using objective markers, namely, CSF-LDH, blood pH, and bilirubin concentration. These measurements were routinely performed in a clinical laboratory at Shanghai Children's Hospital for the purpose of clinical diagnosis and treatments. Investigators for the clinical data analysis and sample collection were double blinded. The clinical data were enrolled by criteria and shown in fig. S1. The results from the clinical data rationalized further investigations of cellular and molecular mechanisms underlying exacerbated neurotoxicity using isolated mouse neurons and brain slices *in vitro* and long-term behavioral impact *in vivo* in mouse models. Mice 4 and 5 weeks old were randomized by gender during behavioral tests followed by 7 days of modeling from P3 to P10. The number of animals per group in all the experiments was determined on the basis of prior literature, power calculation, and experience from our previous studies to ensure enough sample sizes to allow the detection of statistically significant differences.

For the MWM, ABR, fear conditioning, rotarod test, coimmunoprecipitation and Western blotting, and CSF pH measurement in animal models, experimenters were blinded during data acquisition. We also used CHO cells expressing ASIC1a/2a and *Asic1a*^{-/-} mice for mechanistic analyses. All the DNA sequences of plasmid were confirmed. Either male or female mice were used for all experiments. All animals were anesthetized or euthanized by pentobarbital or isoflurane. The number of replicates for each experiment is labeled in all figures or legends.

Statistical analysis

All data were reported as means ± SEM. Two-tailed paired and unpaired Student's *t* test were used where appropriate to examine the statistical significance of the difference between groups of data. Comparisons among multiple groups were analyzed by one-way and two-way analysis of variance (ANOVA) followed by Tukey's multiple comparison tests for post hoc analysis. For clinical data analysis, Spearman correlation test, Wilcoxon rank sum test, and Dunnett T3 test were used to analyze data in the indicated groups. Statistical software SPSS 24.0 was used to analyze all data.

SUPPLEMENTARY MATERIALS

stm.sciencemag.org/cgi/content/full/12/5/30/eaax1337/DC1
Materials and Methods

Fig. S1. Enrollment flow chart for the study population.

Fig. S2. CSF-LDH is not associated with age, gender, and total bilirubin.

Fig. S3. Biophysical and pharmacological properties of I_{ASICs} in MVN neurons.

Fig. S4. Direct cross-talk between bilirubin and ASICs.

Fig. S5. Enhanced membrane depolarization, spike firings by bilirubin-dependent increase in currents mediated by ASICs.

Fig. S6. Potentiated I_{ASICs} by bilirubin had different sensitivities to various inhibitors of ASIC channels in MVN neurons.

Fig. S7. Bilirubin and acid induce cell death in brain slices and CHO cells.

Fig. S8. Exacerbated brain injury in neonatal mice in vivo conditioned by hyperbilirubinemia and intermittent hypoxia-induced acidosis.

Table S1. Detail information for infants with acidosis or hyperbilirubinemia.

Table S2. Free bilirubin concentration in CSF of neonates with hyperbilirubinemia

(14 subjects) by using a fluorescent protein (UnaG)-based detection method.

References (67–73)

[View/request a protocol for this paper from Bio-protocol.](#)

REFERENCES AND NOTES

- S. M. Shapiro, J. W. Conlee, Brainstem auditory evoked potentials correlate with morphological changes in Gunn rat pups. *Hear. Res.* **57**, 16–22 (1991).
- R. F. Spencer, W. T. Shaia, A. T. Gleason, A. Sismanis, S. M. Shapiro, Changes in calcium-binding protein expression in the auditory brainstem nuclei of the jaundiced Gunn rat. *Hear. Res.* **171**, 129–141 (2002).
- H.-B. Ye, H.-B. Shi, J. Wang, D.-L. Ding, D.-Z. Yu, Z.-N. Chen, C.-Y. Li, W.-T. Zhang, S.-K. Yin, Bilirubin induces auditory neuropathy in neonatal guinea pigs via auditory nerve fiber damage. *J. Neurosci. Res.* **90**, 2201–2213 (2012).
- J. F. Watchko, Kernicterus and the molecular mechanisms of bilirubin-induced CNS injury in newborns. *Neuromolecular Med.* **8**, 513–529 (2006).
- J. Liu, J. Long, S. Zhang, X. Fang, Y. Luo, The impact of SLC10B1 genetic polymorphisms on neonatal hyperbilirubinemia: A systematic review with meta-analysis. *J. Pediatr. (Rio J)* **89**, 434–443 (2013).
- P. K. Tiwari, A. Bhatnagar, R. Agarwal, S. Basu, R. Raman, A. Kumar, *UGT1A1* gene variants and clinical risk factors modulate hyperbilirubinemia risk in newborns. *J. Perinatol.* **34**, 120–124 (2014).
- M. Alexandra Brito, R. F. M. Silva, D. Brites, Bilirubin toxicity to human erythrocytes: A review. *Clin. Chim. Acta* **374**, 46–56 (2006).
- M. Kaplan, C. Hammerman, Understanding and preventing severe neonatal hyperbilirubinemia: Is bilirubin neurotoxicity really a concern in the developed world? *Clin. Perinatol.* **31**, 555–575, x (2004).
- S. Gazzini, N. Strazielle, C. Tiribelli, J.-F. Ghersi-Egea, Transport and metabolism at blood–brain interfaces and in neural cells: Relevance to bilirubin-induced encephalopathy. *Front. Pharmacol.* **3**, 89 (2012).
- I. Palmela, H. Sasaki, F. L. Cardoso, M. Moutinho, K. S. Kim, D. Brites, M. A. Brito, Time-dependent dual effects of high levels of unconjugated bilirubin on the human blood–brain barrier lining. *Front. Cell. Neurosci.* **6**, 22 (2012).
- P. A. Denney, D. S. Seidman, D. K. Stevenson, Neonatal hyperbilirubinemia. *N. Engl. J. Med.* **344**, 581–590 (2001).
- D. J. Benos, B. A. Stanton, Functional domains within the degenerin/epithelial sodium channel (Deg/ENaC) superfamily of ion channels. *J. Physiol.* **520** Pt 3, 631–644 (1999).
- J. A. Wemmie, J. Chen, C. C. Askwith, A. M. Hruska-Hageman, M. P. Price, B. C. Nolan, P. G. Yoder, E. Lamani, T. Hoshi, J. H. Freeman Jr., M. J. Welsh, The acid-activated ion channel ASIC contributes to synaptic plasticity, learning, and memory. *Neuron* **34**, 463–477 (2002).
- R. Waldmann, G. Champigny, F. Bassilana, C. Heurteaux, M. Lazdunski, A proton-gated cation channel involved in acid-sensing. *Nature* **386**, 173–177 (1997).
- O. Krishtal, The ASICs: Signaling molecules? Modulators? *Trends Neurosci.* **26**, 477–483 (2003).
- D. Alvarez de la Rosa, P. Zhang, D. Shao, F. White, C. M. Canessa, Functional implications of the localization and activity of acid-sensitive channels in rat peripheral nervous system. *Proc. Natl. Acad. Sci. U.S.A.* **99**, 2326–2331 (2002).
- S. Gründer, M. Pusch, Biophysical properties of acid-sensing ion channels (ASICs). *Neuropharmacology* **94**, 9–18 (2015).
- Z. G. Xiong, X. M. Zhu, X. P. Chu, M. Minami, J. Hey, W. L. Wei, J. F. MacDonald, J. A. Wemmie, M. P. Price, M. J. Welsh, R. P. Simon, Neuroprotection in ischemia: Blocking calcium-permeable acid-sensing ion channels. *Cell* **118**, 687–698 (2004).
- J. Gao, B. Duan, D.-G. Wang, X.-H. Deng, G.-Y. Zhang, L. Xu, T.-L. Xu, Coupling between NMDA receptor and acid-sensing ion channel contributes to ischemic neuronal death. *Neuron* **48**, 635–646 (2005).
- B. Duan, Y.-Z. Wang, T. Yang, X.-P. Chu, Y. Yu, Y. Huang, H. Cao, J. Hansen, R. P. Simon, M. X. Zhu, Z.-G. Xiong, T.-L. Xu, Extracellular spermine exacerbates ischemic neuronal injury through sensitization of ASIC1a channels to extracellular acidosis. *J. Neurosci.* **31**, 2101–2112 (2011).
- J. F. Watchko, C. Tiribelli, Bilirubin-induced neurologic damage—Mechanisms and management approaches. *N. Engl. J. Med.* **369**, 2021–2030 (2013).
- T. W. Sherwood, K. G. Lee, M. G. Gormley, C. C. Askwith, Heteromeric acid-sensing ion channels (ASICs) composed of ASIC2b and ASIC1a display novel channel properties and contribute to acidosis-induced neuronal death. *J. Neurosci.* **31**, 9723–9734 (2011).
- A. Kumagai, R. Ando, H. Miyatake, P. Greimel, T. Kobayashi, Y. Hirabayashi, T. Shimogori, A. Miyawaki, A bilirubin-inducible fluorescent protein from eel muscle. *Cell* **153**, 1602–1611 (2013).
- L. Vitek, L. Muchová, J. Zelenka, M. Zadinová, J. Malina, The effect of zinc salts on serum bilirubin levels in hyperbilirubinemic rats. *J. Pediatr. Gastroenterol. Nutr.* **40**, 135–140 (2005).
- X.-P. Chu, J. A. Wemmie, W.-Z. Wang, X.-M. Zhu, J. A. Saugstad, M. P. Price, R. P. Simon, Z.-G. Xiong, Subunit-dependent high-affinity zinc inhibition of acid-sensing ion channels. *J. Neurosci.* **24**, 8678–8689 (2004).
- X.-L. Yin, M. Liang, H.-B. Shi, L.-Y. Wang, C.-Y. Li, S.-K. Yin, The role of gamma-aminobutyric acid/glycinergic synaptic transmission in mediating bilirubin-induced hyperexcitation in developing auditory neurons. *Toxicol. Lett.* **240**, 1–9 (2016).
- L.-Y. Wang, M. J. Fedchyshyn, Y.-M. Yang, Action potential evoked transmitter release in central synapses: Insights from the developing calyx of Held. *Mol. Brain* **2**, 36 (2009).
- C.-Y. Li, H.-B. Shi, Z.-N. Chen, H.-B. Ye, N.-y. Song, S.-K. Yin, Protein kinase A and C signaling induces bilirubin potentiation of GABA/glycinergic synaptic transmission in rat ventral cochlear nucleus neurons. *Brain Res.* **1348**, 30–41 (2010).
- A. Baron, L. Schaefer, E. Lingueglia, G. Champigny, M. Lazdunski, Zn²⁺ and H⁺ are coactivators of acid-sensing ion channels. *J. Biol. Chem.* **276**, 35361–35367 (2001).
- S. Lilley, P. LeTissier, J. Robbins, The discovery and characterization of a proton-gated sodium current in rat retinal ganglion cells. *J. Neurosci.* **24**, 1013–1022 (2004).
- A. Baron, N. Voilley, M. Lazdunski, E. Lingueglia, Acid sensing ion channels in dorsal spinal cord neurons. *J. Neurosci.* **28**, 1498–1508 (2008).
- A. Baron, E. Deval, M. Salinas, E. Lingueglia, N. Voilley, M. Lazdunski, Protein kinase C stimulates the acid-sensing ion channel ASIC2a via the PDZ domain-containing protein PICK1. *J. Biol. Chem.* **277**, 50463–50468 (2002).
- M. Vukicevic, S. Kellenberger, Modulatory effects of acid-sensing ion channels on action potential generation in hippocampal neurons. *Am. J. Physiol. Cell Physiol.* **287**, C682–C690 (2004).
- L.-J. Wu, B. Duan, Y.-D. Mei, J. Gao, J.-G. Chen, M. Zhuo, L. Xu, M. Wu, T.-L. Xu, Characterization of acid-sensing ion channels in dorsal horn neurons of rat spinal cord. *J. Biol. Chem.* **279**, 43716–43724 (2004).
- T. Hattori, J. Chen, A. M. S. Harding, M. P. Price, Y. Lu, F. M. Abboud, C. J. Benson, ASIC2a and ASIC3 heteromultimerize to form pH-sensitive channels in mouse cardiac dorsal root ganglia neurons. *Circ. Res.* **105**, 279–286 (2009).
- Y.-W. Lin, M.-Y. Min, C.-C. Lin, W.-N. Chen, W.-L. Wu, H.-M. Yu, C.-C. Chen, Identification and characterization of a subset of mouse sensory neurons that express acid-sensing ion channel 3. *Neuroscience* **151**, 544–557 (2008).
- C. J. Benson, J. Xie, J. A. Wemmie, M. P. Price, J. M. Hens, M. J. Welsh, P. M. Snyder, Heteromultimers of DEG/ENaC subunits form H⁺-gated channels in mouse sensory neurons. *Proc. Natl. Acad. Sci. U.S.A.* **99**, 2338–2343 (2002).
- E. Deval, J. Noël, N. Lay, A. Alloui, S. Diochot, V. Friend, M. Jodar, M. Lazdunski, E. Lingueglia, ASIC3, a sensor of acidic and primary inflammatory pain. *EMBO J.* **27**, 3047–3055 (2008).
- A. Buta, O. Maximyuk, D. Kovalsky, V. Sukach, M. Vovk, O. Ievlevskiy, E. Isaeva, D. Isaev, A. Savotchenko, O. Krishtal, Novel potent orthosteric antagonist of ASIC1a prevents NMDAR-dependent LTP induction. *J. Med. Chem.* **58**, 4449–4461 (2015).
- R. L. Levine, W. R. Fredericks, S. I. Rapoport, Clearance of bilirubin from rat brain after reversible osmotic opening of the blood–brain barrier. *Pediatr. Res.* **19**, 1040–1043 (1985).
- R. Brodersen, L. Stern, Deposition of bilirubin acid in the central nervous system—a hypothesis for the development of kernicterus. *Acta Paediatr. Scand.* **79**, 12–19 (1990).
- R. P. Wennberg, S. M. Gospe Jr., W. D. Rhine, M. Seyal, D. Saeed, G. Sosa, Brainstem bilirubin toxicity in the newborn primate may be promoted and reversed by modulating PCO₂. *Pediatr. Res.* **34**, 6–9 (1993).
- S. Zougbedé, F. Miller, P. Ravassard, A. Rebollo, L. Cicerón, P.-O. Couraud, D. Mazier, A. Moreno, Metabolic acidosis induced by *Plasmodium falciparum* intraerythrocytic stages alters blood–brain barrier integrity. *J. Cereb. Blood Flow Metab.* **31**, 514–526 (2011).
- M. Nasralla, E. Gawronska, D. Yi-Yung Hsia, Studies on the relation between serum and spinal fluid bilirubin during early infancy. *J. Clin. Invest.* **37**, 1403–1412 (1958).
- M. J. Daood, J. F. Watchko, Calculated in vivo free bilirubin levels in the central nervous system of Gunn rat pups. *Pediatr. Res.* **60**, 44–49 (2006).
- M. J. Daood, A. F. McDonagh, J. F. Watchko, Calculated free bilirubin levels and neurotoxicity. *J. Perinatol.* **29** Suppl 1, S14–S19 (2009).
- J. B. Posner, F. Plum, Spinal-fluid pH and neurologic symptoms in systemic acidosis. *N. Engl. J. Med.* **277**, 605–613 (1967).

48. İ. Akman, E. Özek, S. Kulekci, D. Türkdog˘an, D. Cebeci, F. Akdaş, Auditory neuropathy in hyperbilirubinemia: Is there a correlation between serum bilirubin, neuron-specific enolase levels and auditory neuropathy? *Int. J. Audiol.* **43**, 516–522 (2004).
49. A. Quaglia, M. Karlsson, M. Larsson, W. R. Taylor, N. T. N. Diep, D. T. Trinh, N. V. Trung, N. Van Kinh, H. F. L. Wertheim, Total lactate dehydrogenase in cerebrospinal fluid for identification of bacterial meningitis. *J. Med. Microbiol.* **62**, 1772–1773 (2013).
50. M. Nussinovitch, Y. Finkelstein, K. P. Elishkevitz, B. Volovitz, D. Harel, G. Klinger, Y. Razon, U. Nussinovitch, N. Nussinovitch, Cerebrospinal fluid lactate dehydrogenase isoenzymes in children with bacterial and aseptic meningitis. *Transl. Res.* **154**, 214–218 (2009).
51. Z.-G. Xiong, R. Raouf, W.-Y. Lu, L.-Y. Wang, B. A. Orser, E. M. Dudek, M. D. Browning, J. F. MacDonald, Regulation of *N*-methyl-D-aspartate receptor function by constitutively active protein kinase C. *Mol. Pharmacol.* **54**, 1055–1063 (1998).
52. F. N. Soria, A. Pérez-Samartin, A. Martin, K. B. Gona, J. Llop, B. Szczupak, J. C. Chara, C. Matute, M. Domercq, Extrasynaptic glutamate release through cystine/glutamate antiporter contributes to ischemic damage. *J. Clin. Invest.* **124**, 3645–3655 (2014).
53. C. C. Askwith, J. A. Wemmie, M. P. Price, T. Rokhlina, M. J. Welsh, Acid-sensing ion channel 2 (ASIC2) modulates ASIC1 H⁺-activated currents in hippocampal neurons. *J. Biol. Chem.* **279**, 18296–18305 (2004).
54. A. Baron, R. Waldmann, M. Lazdunski, ASIC-like, proton-activated currents in rat hippocampal neurons. *J. Physiol.* **539**, 485–494 (2002).
55. Y. Huang, N. Jiang, J. Li, Y.-H. Ji, Z.-G. Xiong, X.-m. Zha, Two aspects of ASIC function: Synaptic plasticity and neuronal injury. *Neuropharmacology* **94**, 42–48 (2015).
56. F. Mayor Jr., J. Díez-Guerra, F. Valdivieso, F. Mayor, Effect of bilirubin on the membrane potential of rat brain synaptosomes. *J. Neurochem.* **47**, 363–369 (1986).
57. E. L. M. Ochoa, R. P. Wennberg, Y. An, T. Tandon, T. Takashima, T. Nguyen, A. Chui, Interactions of bilirubin with isolated presynaptic nerve terminals: Functional effects on the uptake and release of neurotransmitters. *Cell. Mol. Neurobiol.* **13**, 69–86 (1993).
58. M. Liang, X.-L. Yin, H.-B. Shi, C.-Y. Li, X.-Y. Li, N.-Y. Song, H.-S. Shi, Y. Zhao, L.-Y. Wang, S.-K. Yin, Bilirubin augments Ca²⁺ load of developing bushy neurons by targeting specific subtype of voltage-gated calcium channels. *Sci. Rep.* **7**, 431 (2017).
59. G.-Y. Han, C.-Y. Li, H.-B. Shi, J.-P. Wang, K.-M. Su, X.-L. Yin, S.-K. Yin, Riluzole is a promising pharmacological inhibitor of bilirubin-induced excitotoxicity in the ventral cochlear nucleus. *CNS Neurosci. Ther.* **21**, 262–270 (2015).
60. S. Chai, M. Li, J. Lan, Z.-G. Xiong, J. A. Saugstad, R. P. Simon, A kinase-anchoring protein 150 and calcineurin are involved in regulation of acid-sensing ion channels ASIC1a and ASIC2a. *J. Biol. Chem.* **282**, 22668–22677 (2007).
61. N. J. Allen, D. Attwell, Modulation of ASIC channels in rat cerebellar Purkinje neurons by ischaemia-related signals. *J. Physiol.* **543**, 521–529 (2002).
62. J. W. Conlee, S. M. Shapiro, S. B. Churn, Expression of the α and β subunits of Ca²⁺/calmodulin kinase II in the cerebellum of jaundiced Gunn rats during development: A quantitative light microscopic analysis. *Acta Neuropathol.* **99**, 393–401 (2000).
63. C.-Y. Li, H.-B. Shi, N.-Y. Song, S.-K. Yin, Bilirubin enhances neuronal excitability by increasing glutamatergic transmission in the rat lateral superior olive. *Toxicology* **284**, 19–25 (2011).
64. H.-B. Shi, Y. Kakazu, S. Shibata, N. Matsumoto, T. Nakagawa, S. Komune, Bilirubin potentiates inhibitory synaptic transmission in lateral superior olive neurons of the rat. *Neurosci. Res.* **55**, 161–170 (2006).
65. S. M. Shapiro, Chronic bilirubin encephalopathy: Diagnosis and outcome. *Semin. Fetal Neonatal Med.* **15**, 157–163 (2010).
66. J. F. Ennever, A. T. Costarino, R. A. Polin, W. T. Speck, Rapid clearance of a structural isomer of bilirubin during phototherapy. *J. Clin. Invest.* **79**, 1674–1678 (1987).
67. W.-Z. Zeng, D.-S. Liu, B. Duan, X.-L. Song, X. Wang, D. Wei, W. Jiang, M. X. Zhu, Y. Li, T.-L. Xu, Molecular mechanism of constitutive endocytosis of Acid-sensing ion channel 1a and its protective function in acidosis-induced neuronal death. *J. Neurosci.* **33**, 7066–7078 (2013).
68. O. Mesner, M. J. Miller, S. C. Iben, K. C. Prabha, C. A. Mayer, M. A. Haxhiu, R. J. Martin, Hyperbilirubinemia diminishes respiratory drive in a rat pup model. *Pediatr. Res.* **64**, 270–274 (2008).
69. A.-M. Park, H. Nagase, S. Vinod Kumar, Y. J. Suzuki, Acute intermittent hypoxia activates myocardial cell survival signaling. *Am. J. Physiol. Heart Circ. Physiol.* **292**, H751–H757 (2007).
70. C. V. Vorhees, M. T. Williams, Morris water maze: Procedures for assessing spatial and related forms of learning and memory. *Nat. Protoc.* **1**, 848–858 (2006).
71. Q. Wang, Q. Wang, X.-L. Song, Q. Jiang, Y.-J. Wu, Y. Li, T.-F. Yuan, S. Zhang, N.-J. Xu, M. X. Zhu, W.-G. Li, T.-L. Xu, Fear extinction requires ASIC1a-dependent regulation of hippocampal-prefrontal correlates. *Sci. Adv.* **4**, eaau3075 (2018).
72. B. Li, X.-Y. Zhang, A.-H. Yang, X.-C. Peng, Z.-P. Chen, J.-Y. Zhou, Y.-S. Chan, J.-J. Wang, J.-N. Zhu, Histamine increases neuronal excitability and sensitivity of the lateral vestibular nucleus and promotes motor behaviors via HCN channel coupled to H2 receptor. *Front. Cell. Neurosci.* **10**, 300 (2016).
73. R. Heskin-Sweezie, H. K. Tittley, J. S. Baizer, D. M. Broussard, Type B GABA receptors contribute to the restoration of balance during vestibular compensation in mice. *Neuroscience* **169**, 302–314 (2010).

Acknowledgments: We thank B. Orser and A. Fekete for the constructive comments and Y.-Y. Xia for the many helpful inputs in the statistical analysis of the clinical datasets. **Funding:** This work was supported by the National Natural Science Foundation of China (81720108010 and 81530029 to S.-K.Y., 81730095 to T.-L.X., and 81870722 and 81570909 to H.-B.S.), the Science and Technology Commission of Shanghai Municipality and the Innovative Research Team of High-level Local Universities in Shanghai (18JC1420302 to T.-L.X.), the Shanghai Municipal Education Commission–Gaofeng Clinical Medicine Grant Support (20152233 to H.-B.S.), the Shanghai Outstanding Academic Leaders Plan (2017062 to H.-B.S.), and the Canadian Institutes of Health Research (MOP-81159, MOP-77610, PJT-156034, and PJT-156439 to L.-Y.W.). **Author contributions:** K.L., X.-L.S., and H.-S.S. carried out experiments in vitro and collected the data. X.Q., J.F., and F.W. performed the animal modeling experiments and collected data. K.N. and W.-P.L. collected clinical data. X.-Y.L. supervised the data collection. C.-Y.L. contributed to the pilot experiments and data analyses. O.M. and O.K. provided the compound 5b. T.-L.X. provided *Asic1a* null mice and all the plasmids, as well as intellectual inputs to experiments and writing. H.-B.S., S.-K.Y., and L.-Y.W. designed this study and contributed to the manuscript revisions. L.-Y.W. supervised the experiments and wrote the manuscript with K.L. **Competing interests:** The authors declare that they have no competing interests. **Data and materials availability:** All data associated with this study are present in the paper or the Supplementary Materials.

Submitted 25 February 2019
Resubmitted 3 August 2019
Accepted 10 December 2019
Published 12 February 2020
10.1126/scitranslmed.aax1337

Citation: K. Lai, X.-L. Song, H.-S. Shi, X. Qi, C.-Y. Li, J. Fang, F. Wang, O. Maximyuk, O. Krishtal, T.-L. Xu, X.-Y. Li, K. Ni, W.-P. Li, H.-B. Shi, L.-Y. Wang, S.-K. Yin, Bilirubin enhances the activity of ASIC channels to exacerbate neurotoxicity in neonatal hyperbilirubinemia in mice. *Sci. Transl. Med.* **12**, eaax1337 (2020).

Bilirubin enhances the activity of ASIC channels to exacerbate neurotoxicity in neonatal hyperbilirubinemia in mice

Ke Lai, Xing-Lei Song, Hao-Song Shi, Xin Qi, Chun-Yan Li, Jia Fang, Fan Wang, Oleksandr Maximyuk, Oleg Krishtal, Tian-Le Xu, Xiao-Yan Li, Kun Ni, Wan-Peng Li, Hai-Bo Shi, Lu-Yang Wang and Shan-Kai Yin

Sci Transl Med **12**, eaax1337.
DOI: 10.1126/scitranslmed.aax1337

Targeting acidity in jaundice

Neonatal hyperbilirubinemia, also called jaundice, is a pediatric condition caused by high bilirubin levels. When associated with acidosis, jaundice can trigger neurotoxicity and lead to neurological impairments. Now, Lai *et al.* investigated the link between acidosis and jaundice in human samples and animal models. In samples from children with concomitant acidosis and jaundice, neuronal injury was increased compared with children with jaundice and no acidosis. In mice, bilirubin potentiated the activity of acid-sensing ion channels (ASICs) in neurons, increased firing, and caused cell death. Hyperbilirubinemia and acidosis promoted cognitive impairments in mice that were prevented by ASIC deletion. Targeting ASICs might reduce neurological impairments associated with jaundice.

ARTICLE TOOLS

<http://stm.sciencemag.org/content/12/530/eaax1337>

SUPPLEMENTARY MATERIALS

<http://stm.sciencemag.org/content/suppl/2020/02/10/12.530.eaax1337.DC1>

RELATED CONTENT

<http://stm.sciencemag.org/content/scitransmed/11/512/eaaw3639.full>
<http://stm.sciencemag.org/content/scitransmed/10/470/eaau1643.full>
<http://stm.sciencemag.org/content/scitransmed/10/454/eaan1230.full>
<http://stm.sciencemag.org/content/scitransmed/11/475/eaau7975.full>

REFERENCES

This article cites 73 articles, 17 of which you can access for free
<http://stm.sciencemag.org/content/12/530/eaax1337#BIBL>

PERMISSIONS

<http://www.sciencemag.org/help/reprints-and-permissions>

Use of this article is subject to the [Terms of Service](#)

Science Translational Medicine (ISSN 1946-6242) is published by the American Association for the Advancement of Science, 1200 New York Avenue NW, Washington, DC 20005. The title *Science Translational Medicine* is a registered trademark of AAAS.

Copyright © 2020 The Authors, some rights reserved; exclusive licensee American Association for the Advancement of Science. No claim to original U.S. Government Works